Study on incipient melting in cast Ni base IN939 superalloy during solution annealing and its effect on hot workability

M. R. Jahangiri*[1,2], S. M. A. Boutorabi[1,3] and H. Arabi[1,3]

Incipient melting of IN939 superalloy was investigated during solution annealing. In addition, the effect of this phenomenon was studied on hot workability of the alloy. The incipient melting was detected to be within the temperature range 1150–1160°C, which has been reported to be the standard temperature range of solution annealing of this material. The local melted regions were enriched in Zr, Nb and B elements, which appeared in the form of three different phases. The results also showed that even small amounts of local melted regions impair hot workability of the alloy. The use of long time solution annealing at 1150°C or a two-step solution heat treatment has been recommended to delay the incipient melting of the alloy. These treatments enhance hot workability of the alloy.

Keywords: IN939 superalloy, Incipient melting, Solution annealing, DSC, Hot workability

Introduction

Hot components of gas turbines are degraded during service, because they work under hard conditions including high mechanical/thermal stresses at elevated temperatures. Blades and vanes are among the most important and expensive components of a gas turbine. Nickel or cobalt base superalloys are used in the manufacturing of these components to withstand high temperatures and exhibit little microstructural changes during service.[1–4]

IN939 superalloy is one of the cast alloys designed by the company 'Inco' for long lifetime and for higher resistance to corrosion at temperatures up to ~850°C. This alloy has been developed for use in the manufacturing of gas turbine blades and vanes, fuel nozzles, retaining rings, diffusers and other structural components.[5–10]

In order to provide the appropriate creep properties at temperatures higher than 800°C and for access to desirable tensile properties in a wide range of temperatures, the heat treatment of the alloy is performed in four stages that is known as 'standard four-stage heat treatment'. The four stages of this heat treatment are as follows,[5,6,10] in which FAC is the abbreviation of 'fast air cooling' and 'air cooling' is abbreviated as AC: 1160°C (4 h)/FAC + 1000°C (6 h)/FAC + 900°C (24 h)/AC + 700°C (16 h)/AC.

Other heat treatment procedures are also stated in published reports;[8,9,11,12] all of them contain the solution annealing cycle at a temperature range 1150–1160°C for 4 h. The aim of this cycle is the full solution of γ' and η phases in the microstructure of cast alloy and homogenisation of the material to procure optimised mechanical properties after heat treatment.[5,13]

The first stage of heat treatment for most of the precipitation hardened Ni based superalloys is the solution annealing as in the case of IN939 alloy. This process, which can be selected as partial or full solution annealing, would have a significant effect on the microstructure and mechanical properties of the alloys. To provide more homogenised microstructure and better creep properties, higher temperatures of solution annealing are used; however, this can lead to a reduction of other properties such as thermal fatigue resistance and tensile strength.[1,2]

Selection of appropriate temperature for full solution annealing of γ' precipitates in the microstructure of cast parts is very difficult due to the segregation of different alloying elements (especially Ti and Al) on different areas of dendrite cores or interdendritic regions. This produces γ' phases with different chemical composition at various regions of the microstructure, which would lead to different solution temperatures.

The microscopic segregations are said to be produced as a result of non-equilibrium solidification of the alloy. They are particularly created for cast components having larger cross-sections with slower solidification rates. Consequently, the precise selection of solution annealing process for these castings is very complex. In addition to the matrix and γ' phases, most superalloys have other important phases such as γ–γ' eutectics, MC carbides, TCP phases, η phase and borides. The presence of these phases and the effect of solution annealing

[1]School of Metallurgy and Materials Engineering, Iran University of Science and Technology, Tehran 16846-13114, Iran
[2]Metallurgy Department, Niroo Research Institute, Tehran 14686, Iran
[3]Center of Excellence for Advanced Materials and Processing, Iran University of Science and Technology, Tehran, Iran

*Corresponding author, email jahangiri@iust.ac.ir

Published by Maney on behalf of the Institute
Received 1 May 2012; accepted 20 July 2012
DOI 10.1179/1743284712Y.0000000090

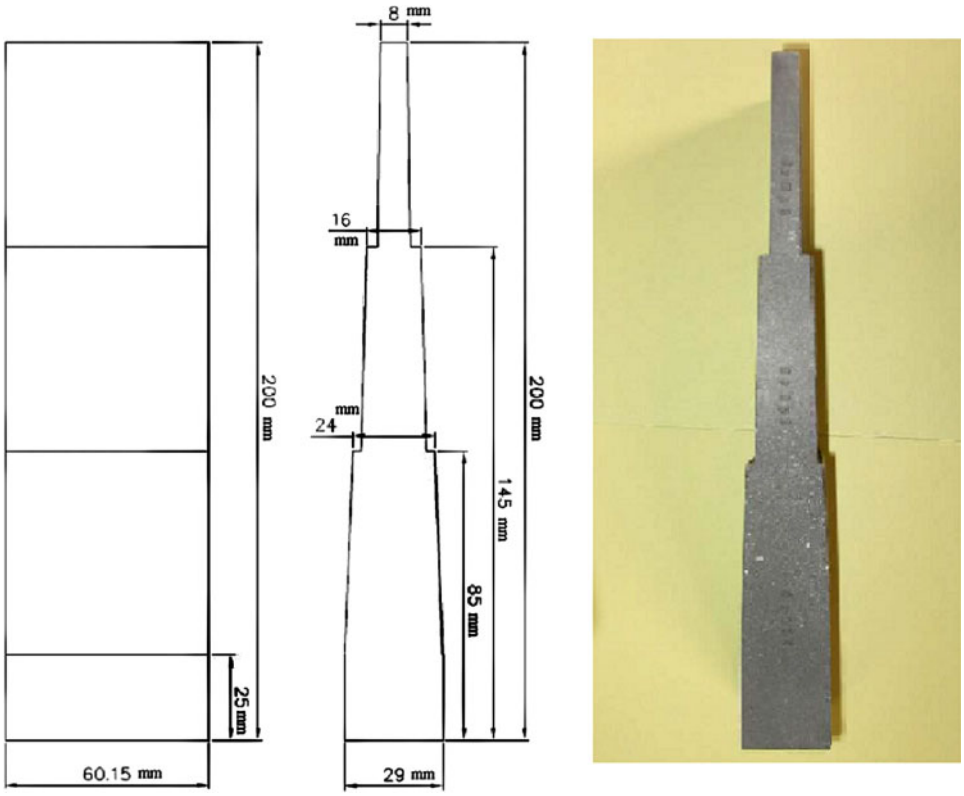

1 Drawing of cast mould and example of cast components

temperature on their morphology and content can add further difficulties to select optimised solution annealing conditions. For example, even though the complete dissolution temperature for γ' particles in IN738 superalloy is >1170°C,[14–16] in practice, the standard solution annealing is performed at 1120°C due to the incipient melting of the alloy. In addition, for IN939 alloy, though the complete dissolution temperature of γ' particles has been reported to be in the temperature range 1080–1100°C,[5,13] the solution annealing for this alloy in practice is at a temperature range 1150–1160°C because of the need for complete dissolution of η phase.

While for many of the polycrystalline, directional solidified or single crystal superalloys, the upper range of solution annealing temperature is restricted by the incipient melting temperature,[17–19] there are no published data about the actual incipient melting point of IN939 superalloy.

Thus, the objectives of the present work are to evaluate the incipient melting of IN939 superalloy and to investigate the possibility of reducing or eliminating this phenomenon by application of a modified heat treatment route. Moreover, the effect of local melting that occurs during annealing process was investigated on the hot workability of the alloy.

Experimental

Master ingots of IN939 superalloy were melted in a vacuum induction furnace. The melt was poured in ceramic moulds under vacuum of 10^{-3} mbar. Pouring temperature was 1460°C, and the mould preheating temperature was 1050°C.

The moulds were designed to achieve three different solidification rates. Figure 1 shows the sketch of the cast parts and also an example of the castings.

From a heavier section of the castings, suitable sample was prepared for differential scanning calorimetry (DSC) test. The heating of the specimen from room temperature to 1400°C was performed at a rate of 10°C min^{-1} under argon atmosphere. Furthermore, adequate specimens were cut from cast parts and heat treated at a temperature range 1100–1250°C for 2–24 h. Then, the specimens were water quenched. Dimensions of the heat treated specimens were $10 \times 10 \times 10$ mm. The specimens were prepared for metallography by conventional grinding and polishing procedures and etched either chemically by a solution of 0·3 g MoO_3 + 10 mL HNO_3 + 10 mL HCl + 15 mL water or electrolytically in 10% oxalic acid at 3 V for 10 s. Their microstructures were investigated by both optical microscopy and scanning electron microscopy (SEM) techniques. The SEM was equipped with an energy dispersive X-ray spectrometer (EDS) system.

Results and discussion

Cast conditions

The chemical composition of the IN939 alloy used in present work is Ni–0·144C–19·25Co–22·38Cr–3·65Ti–1·99Al–1·97W–1·45Ta–0·99Nb–0·09Zr–0·011B–0·002P–0·001S (wt-%). Figures 2 and 3 show the microstructures of the specimens taken from the small and the large cross-section segments of castings respectively. The results show that the cast microstructures are entirely dendritic. Secondary dendrite arm spacing for the larger cross-section segments was about two times higher than that of the smaller cross-section segments. The microstructure of the cast parts includes the matrix γ together with the other precipitated phases such as γ' particles, MC carbides and some other platelet shape phases.

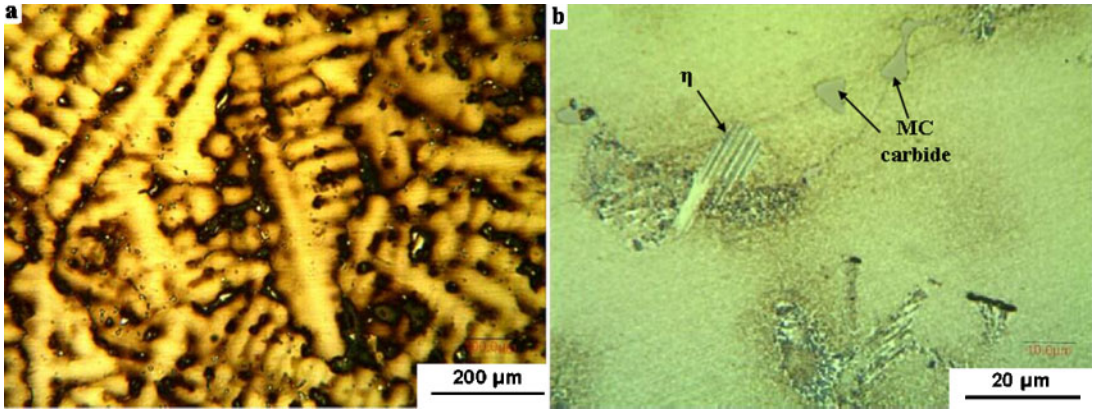

2 Microstructure of specimens taken from small cross-section segments of castings

To examine the segregation of different elements in the cast parts, the specimens were analysed by point or line EDS. Figure 4 shows an example of the results obtained. It is found that elements Ti, Nb and Zr are the main positive segregating elements and Cr is the main negative segregating element. Al does not segregate clearly. This segregation behaviour of the alloying elements has been observed in other cast superalloys;[20–23] however, a considerable Al segregation has been reported for other Ni based superalloys,[24–25] which cannot be seen in IN939 superalloy.

The results of X-ray diffraction and EDS analyses for identification of the phases in the as cast microstructure are presented in Figs. 5 and 6. The results show that the η (point A in Fig. 6) and MC type carbide (point C in Fig. 6) are present in the cast samples. Typical chemical compositions of these phases are given in Fig. 6.

Solution annealed conditions

Knowledge of the incipient melting temperature is critical to the control of superalloy processing and its utilisation. One of the appropriate methods to study the effects of heat treatment on the microstructural features of IN939 superalloy, especially its incipient melting temperature, is thermal analysis (i.e. differential thermal analysis and DSC). The usefulness of this method to characterise the critical temperatures of various superalloys has been demonstrated elsewhere;[26–28] nevertheless, little data have been published for IN939 alloy.

Figure 7*a* shows DSC thermogram for IN939 sample taken from the large cross-section castings at the temperature range 850–1400°C. For better determination of the critical temperatures, the derivative of heat flow with respect to time (dynamic DSC) should be also given. Figure 7*b* shows a zoom of the DSC thermogram at the temperature range 1100–1300°C.

Figure 7 indicates that there is an endothermic peak within the temperature range 1160–1168°C. Another endothermic peak occurs at the temperature range 1193–1344°C. The broad peak refers to general melting process, which begins at a moderate rate at 1193°C and a stronger rate at 1259°C. This finally terminates to liquidus temperature of the alloy at 1344°C. Inflection on the DSC thermogram during the general melting (at 1315–1322°C) comes from the dissolution of the MC carbides as reported[26] for other superalloys. Comparing the measured critical temperatures to the scarce published data[5,29] indicates that there is no prior report about the first (narrow) endothermic peak at the temperature range 1160–1168°C.

The solidus temperature of the alloy has been reported at 1235°C.[5] This temperature, which has been obtained during the solidification experiments (cooling thermograms), can be compared with the temperature of 1259°C measured in the present work. The difference in these values might have been arisen from the need to some amount of undercooling during solidification. As mentioned earlier, 1259°C is the starting point of the general melting of the alloy with a strong rate. Thus, it appears that the published data did not sufficiently pay attention to the incipient melting of the alloy. This is especially important, because the standard solution cycle

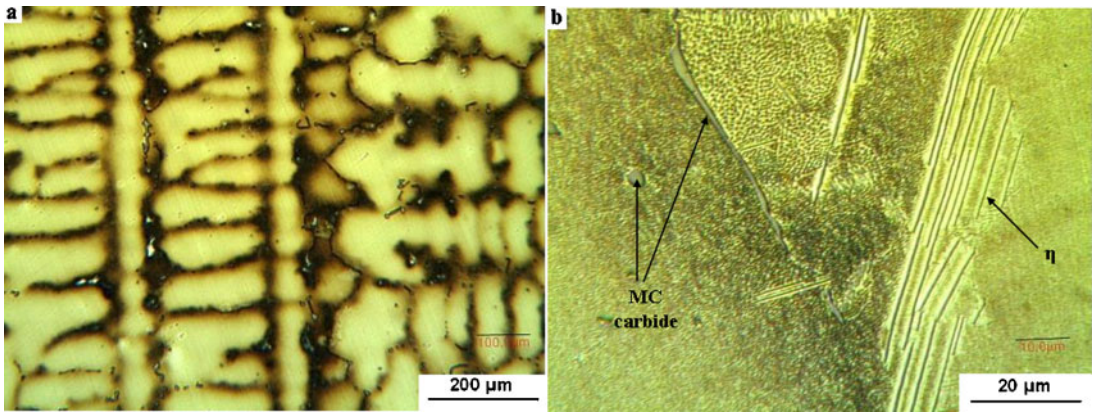

3 Microstructure of specimens taken from large cross-section segments of castings

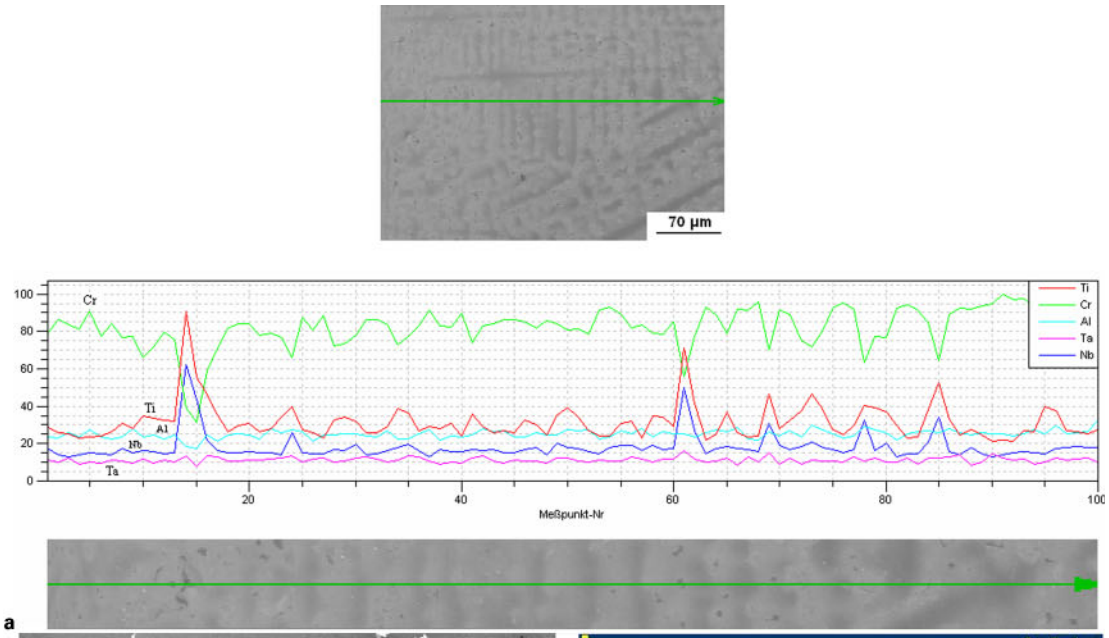

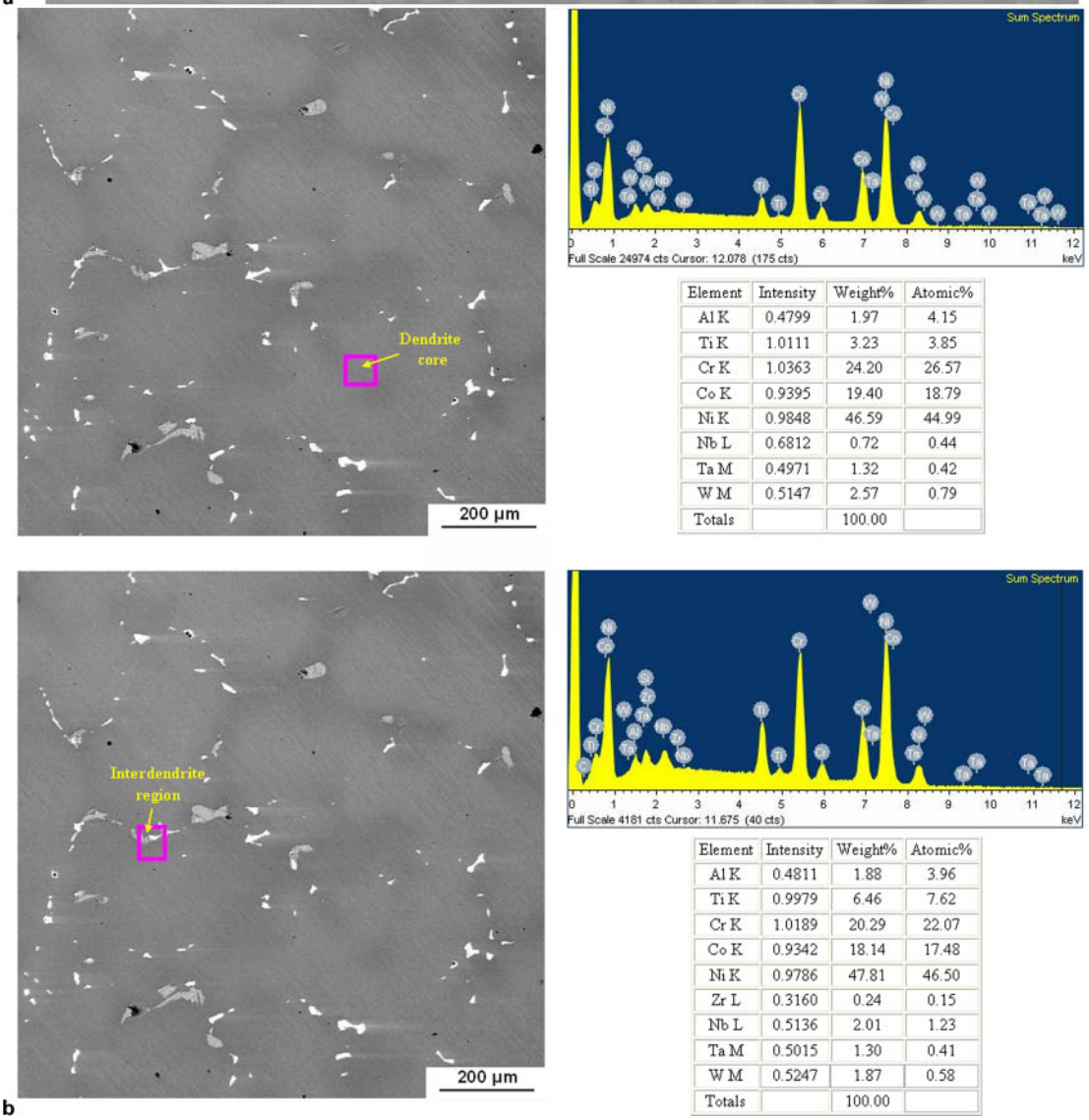

Element	Intensity	Weight%	Atomic%
Al K	0.4799	1.97	4.15
Ti K	1.0111	3.23	3.85
Cr K	1.0363	24.20	26.57
Co K	0.9395	19.40	18.79
Ni K	0.9848	46.59	44.99
Nb L	0.6812	0.72	0.44
Ta M	0.4971	1.32	0.42
W M	0.5147	2.57	0.79
Totals		100.00	

Element	Intensity	Weight%	Atomic%
Al K	0.4811	1.88	3.96
Ti K	0.9979	6.46	7.62
Cr K	1.0189	20.29	22.07
Co K	0.9342	18.14	17.48
Ni K	0.9786	47.81	46.50
Zr L	0.3160	0.24	0.15
Nb L	0.5136	2.01	1.23
Ta M	0.5015	1.30	0.41
W M	0.5247	1.87	0.58
Totals		100.00	

a line scan through dendritic microstructure; *b* point analysis of dendrite cores and interdendritic regions

4 Typical EDS analysis used to investigate segregation of alloying elements in cast parts

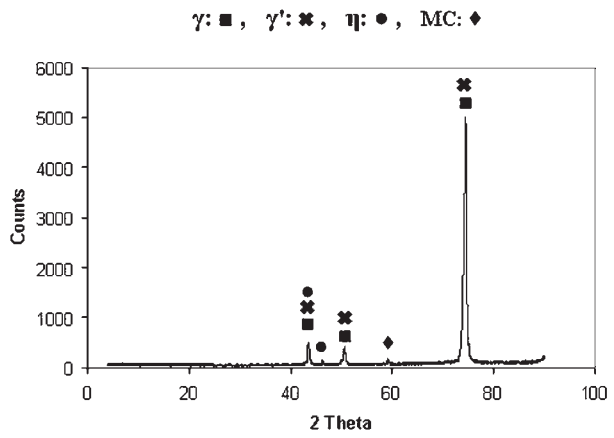

5 X-ray diffraction analysis of large cross-section castings

during heat treatment of the alloy is performed at the temperature range 1150–1160°C, which is extremely close to the first endothermic peak of the alloy that seems to be a representation of its incipient melting point. The nature of this incipient melting process cannot be demonstrated solely by DSC data and should be confirmed by practical heat treatments and metallographic investigation. In fact, DSC is an indirect method of examining phase transformations. Therefore, there is always a need to combine the DSC technique with the other direct experimental methods, such as metallographic examinations, to establish the incipient melting point with greater confidence.

As mentioned in the section on 'Experimental', a series of the cast samples were heated to various temperatures (i.e. 1100–1250°C). After reaching the specified temperature, the samples were hold for 2–24 h and subsequently water quenched. Therefore, the critical temperatures measured by DSC and/or determined by metallography technique can be compared.

Figures 8–11 show the microstructures and analysis of some important phases detected in the specimens annealed at different temperatures. Figure 8 shows that at 1100°C, although most of the γ' particles were dissolved, there were still some of these precipitates in the interdendritic regions beside MC carbides and η phase. There is no evidence of incipient melting in the microstructure.

With increasing annealing temperature from 1100 to 1125°C, the γ' phase was completely dissolved, but η phase was still observed in the microstructure. At 1150°C, local (incipient) melting occurred during annealing of the alloy. As shown in Fig. 9, incipient melting was initiated around the existing η phase in the interdendritic regions. Consequently, the practical incipient melting temperature of the IN939 superalloy was estimated to be between 1125 and 1150°C. This is at least 10°C less than that obtained by the DSC method.

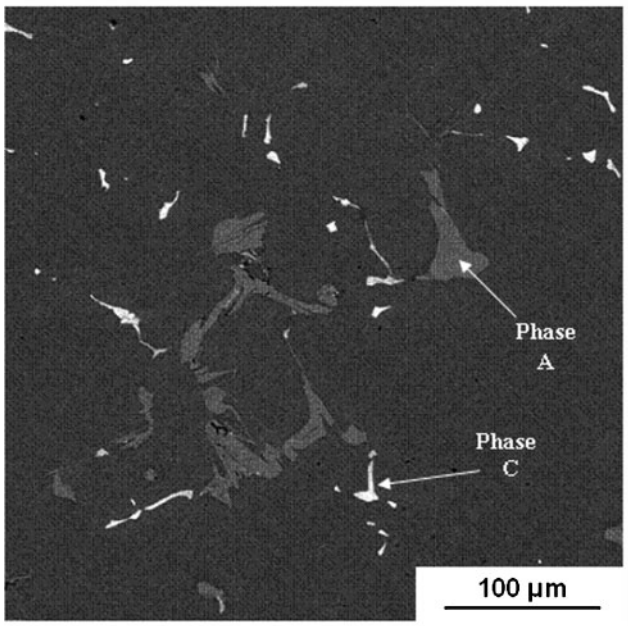

EDS analysis of Phase A

Element	App Conc.	Intensity Corrn.	Weight%	Weight% Sigma	Atomic%
Al K	6.49	0.4482	2.20	0.24	4.45
Si K	4.58	0.5645	1.23	0.21	2.40
Ti K	91.43	0.9841	14.11	0.30	16.09
Cr K	20.40	1.0153	3.05	0.22	3.21
Co K	86.79	0.9446	13.95	0.44	12.93
Ni K	424.95	0.9858	65.46	0.54	60.92
Totals			100.00		

EDS analysis of Phase C

Element	App Conc.	Intensity Corrn.	Weight%	Weight% Sigma	Atomic%
C K	35.74	0.4026	11.16	3.50	45.68
S K	0.94	0.7669	0.15	0.30	0.24
Ti K	138.80	0.9138	19.10	0.87	19.60
Cr K	36.99	0.9330	4.98	0.37	4.71
Co K	28.07	0.9691	3.64	0.41	3.04
Ni K	88.70	1.0215	10.92	0.67	9.14
Nb L	83.43	0.6733	15.58	0.92	8.24
Ta M	210.60	0.7686	34.45	1.53	9.36
Totals			100.00		

6 Image (SEM) with EDS analysis of some phases in microstructure of cast alloy

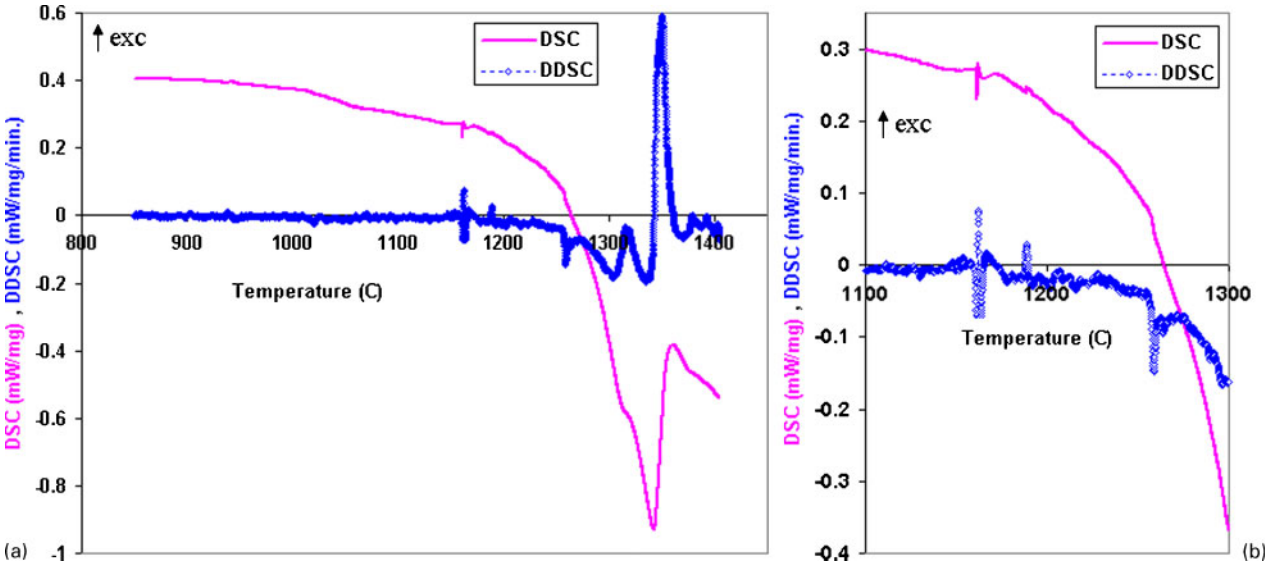

a at temperature range 850–1400°C; *b* zoom of DSC thermogram at temperature range 1100–1300°C

7 Differential scanning calorimetry thermogram for IN939 sample taken from large cross-section castings

The reason of this difference is the higher heating rates used in the heat treatment process, which was established by metallography technique. In effect, the higher heating rate is associated with shorter time for chemical diffusion of segregating elements. Consequently, one can say that the practical incipient melting temperature determined by metallographical method lies below that measured by DSC test.

As stated earlier, since the standard solution treatment of the IN939 alloy is conducted at the temperature range 1150–1160°C, the incipient melting observed at this temperature range should be noticed with a great

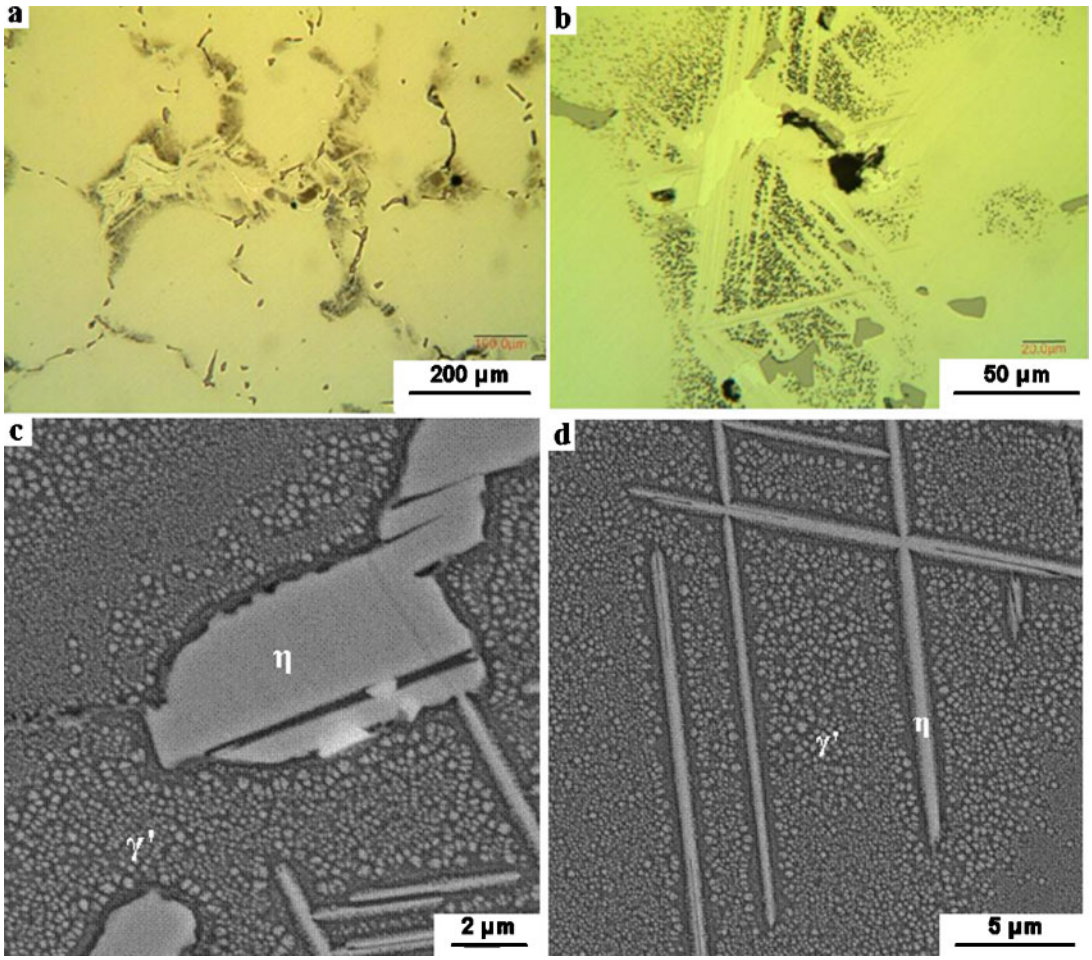

a, *b* optical microstructures with different magnifications; *c*, *d* SEM microstructure from different locations of specimens

8 Microstructure of specimens annealed at 1100°C for 4 h followed by water quenching

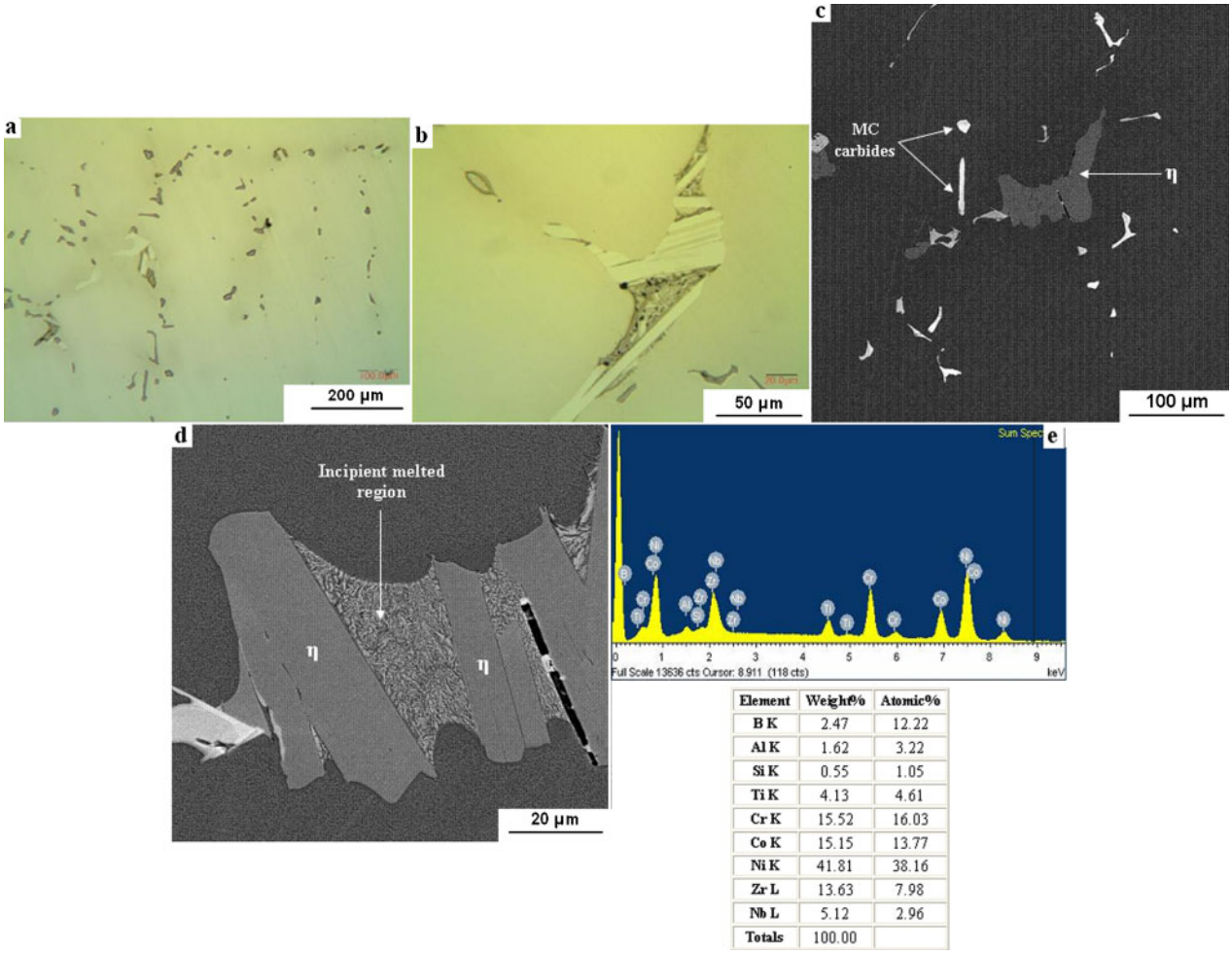

Element	Weight%	Atomic%
B K	2.47	12.22
Al K	1.62	3.22
Si K	0.55	1.05
Ti K	4.13	4.61
Cr K	15.52	16.03
Co K	15.15	13.77
Ni K	41.81	38.16
Zr L	13.63	7.98
Nb L	5.12	2.96
Totals	100.00	

a, *b* optical microstructures with different magnifications; *c*, *d* SEM microstructures with different magnifications; *e* EDS analysis of incipient melted region

9 Microstructure of specimens annealed at 1150°C for 4 h followed by water quenching

care. This observation has not been published so far for IN939 superalloy.

Analysis by EDS showed that these local melted regions are rich in elements Zr and B and to some extent in Nb and Ti (Fig. 9). Analysis of several incipient melted regions near the η phase showed that the overall composition of these regions is as follows, in which the subscripts represent the atomic percentage of related elements ($Ni_{30–45}$, $Co_{10–16}$, $Cr_{15–30}$) ($Zr_{7–11}$, $Nb_{3–7}$, $Ti_{4–8}$, B, Si, Al)

Three distinct phases were observed at these local melted regions (Fig. 10). One of these phases contained high amount of Zr and some Cr, Ti and Nb elements. Another phase was enriched in Cr and B, and the third one was rich in Ti, which was similar to the composition of η phase. The phase enriched in Zr had a composition near the eutectic point of the (Ni–Co)–Zr system, which has an easy glass forming (amorphisation) ability according to Refs. 30–33. The segregation of alloying elements such as B and Zr can promote the incipient melting phenomenon in Ni base superalloys during solution annealing or welding according to Refs. 34–37, because these elements can decrease the local melting temperature of the alloy.

With further increasing of the annealing temperature to a temperature range 1200–1250°C, the volume fraction of these incipient melted regions increased (Fig. 11*a*–*e*). Figure 11*f* shows that the melting of the alloy expanded and the growth of these melted regions was in a honeycomb form.

Microstructural examinations of various specimens annealed for 2–24 h at 1150°C showed that even after 24 h at 1150°C, there were some η phase in the microstructure (Fig. 12*a*–*c*). The important point was the disappearance of the incipient melting after annealing at 1150°C for longer than 16 h (Fig. 12*b*). It seems that the longer annealing time causes the segregated elements to diffuse far from the incipient melted regions, and this leads to disappearance of these regions.

The results of the present research showed that using a two-step heat treatment, first annealing at the temperature range 1100–1150°C for at least 16 h followed by annealing at 1200°C for no less than 10 h, ensures entire dissolution of the η phase without the presence of any residual incipient melting (Fig. 12*e*). The first stage provided suitable conditions for low melting segregated elements to go away from the η phase and distributed them in the microstructure more uniformly, and the second stage of annealing at 1200°C completely dissolved the remainder of the η phase without any occurrence of the localised incipient melting. This seems to be due to the homogenisation of the microstructure in the previous stage of annealing.

Using a one-stage heat treatment at high temperatures, for example 1200°C, for longer times is prohibited

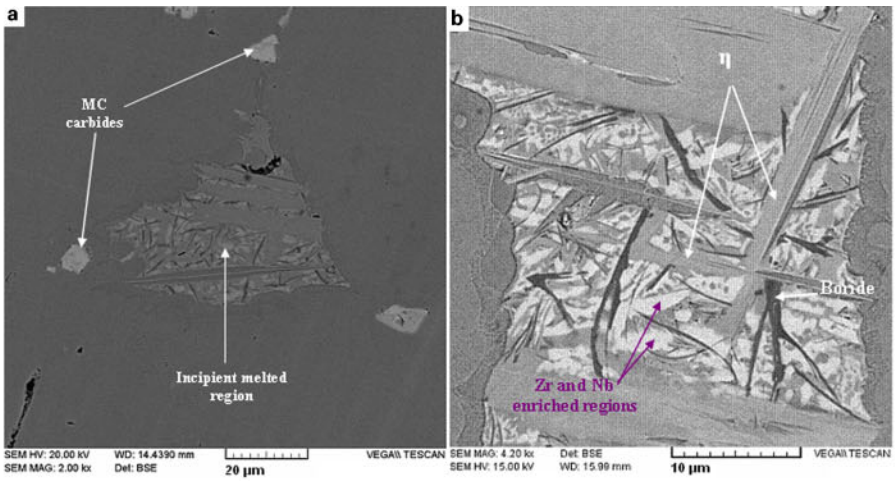

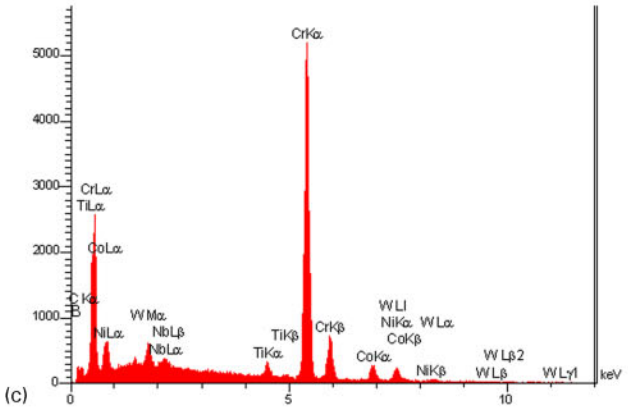

Element	Line	W%	A%
B	Ka	33.73	62.81
C	Ka	9.68	16.23
Ti	Ka	1.22	0.51
Cr	Ka	44.36	17.18
Co	Ka	4.21	1.44
Ni	Ka	4.22	1.45
Nb	La	0.96	0.21
W	La	1.61	0.18
		100.00	100.00

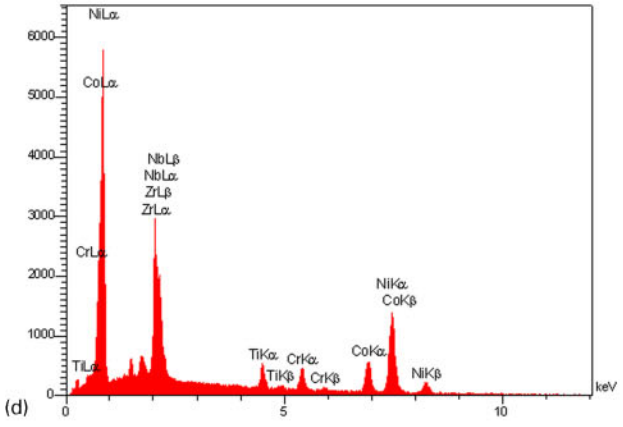

Element	Line	W%	A%
Ti	Ka	4.04	5.41
Cr	Ka	5.12	6.31
Co	Ka	14.78	16.07
Ni	Ka	48.38	52.81
Zr	La	22.99	16.15
Nb	La	4.70	3.24
		100.00	100.00

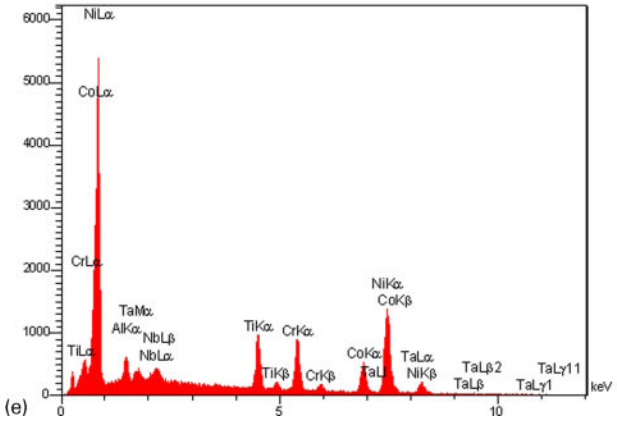

Elementt	Line	W%	A%
Al	Ka	2.74	5.66
Ti	Ka	11.79	14.54
Cr	Ka	12.85	13.47
Co	Ka	14.70	13.84
Ni	Ka	54.09	50.45
Nb	La	2.75	1.71
Ta	La	1.08	0.33
		100.00	100.00

a, *b* SEM microstructures with different magnifications; *c*–*e* EDS analysis of three different phases

10 Microstructure of specimens annealed at 1150°C for 4 h followed by water quenching showing three distinct phases in incipient melted regions

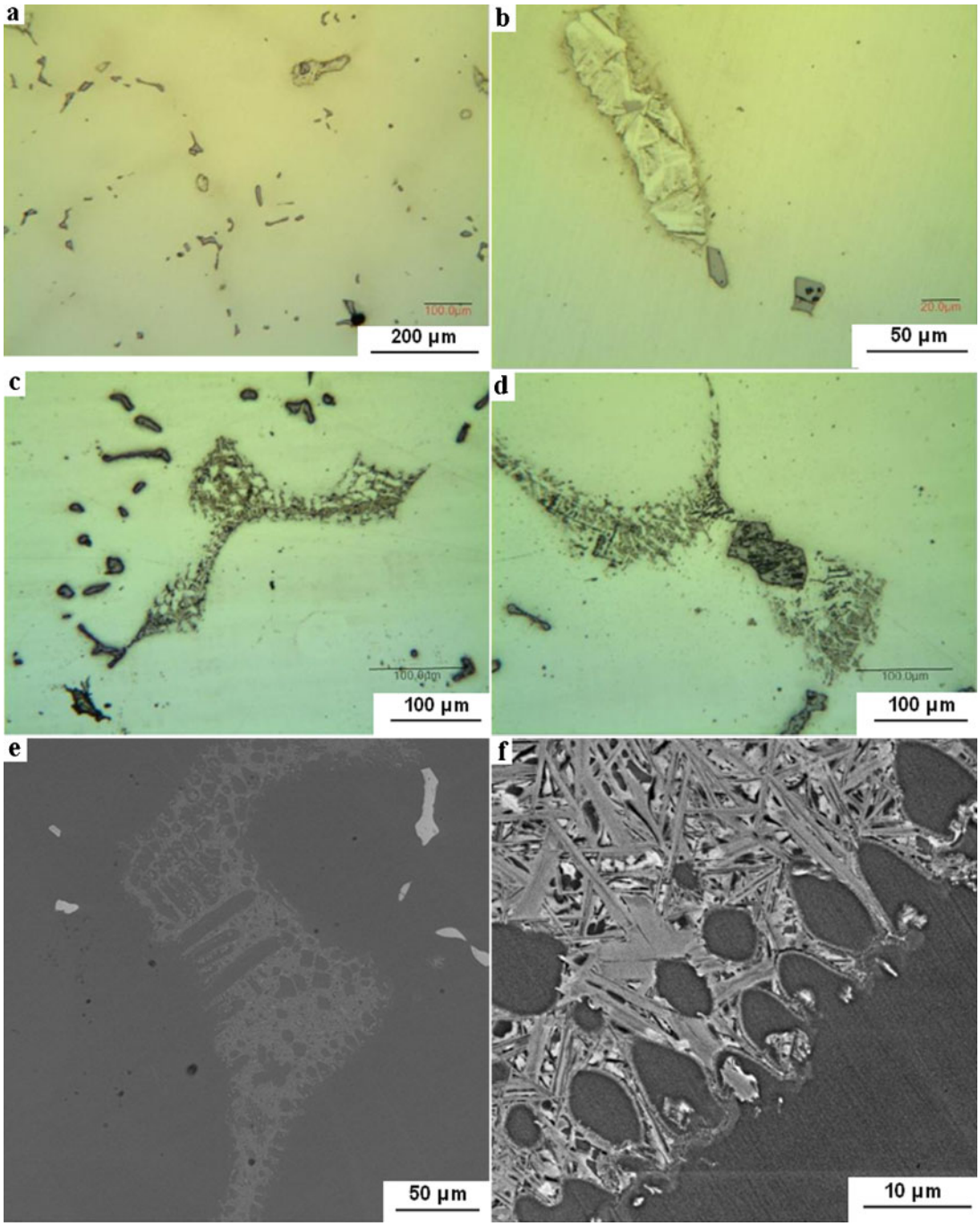

a, *b* 1200°C, optical microstructures with different magnifications; *c*, *d* 1250°C, optical microstructures with different magnifications; *e*, *f* 1250°C, SEM microstructures with different magnifications showing honeycomb growth of melted zones

11 Microstructure of specimens annealed at 1200–1250°C for 4 h followed by water quenching

because of the formation of large amounts of incipient melted regions in the microstructure despite the complete dissolution of the η phase (Fig. 12*f*).

Effect of incipient melting on hot workability

It has been well known that the incipient melting and the presence of even a small fraction of liquid can lead to hot tearing phenomenon in most metals especially superalloys during hot working.[26,38] To study the importance of the incipient melting during hot working of IN939 superalloy, three sets of specimens cut from the large cross-section of the cast bars were hot rolled at 1150°C via five passes; each of which reduced the thickness by ~10%. The specimens were reheated at 1150°C between each pass to maintain the temperature. The first set of specimens were annealed at 1150°C for 4 h before hot rolling, while the second set of specimens were annealed at 1150°C for 24 h. The third set of specimens were initially annealed at 1125°C for 20 h followed by annealing at 1200°C for 10 h.

Figure 13 shows the hot rolled strips produced from each set of specimens. For the specimens that contained incipient melted regions (i.e. first set), severe cracking occurred after the second pass of the hot rolling so that it was impossible to continue the rolling procedure. On the other hand, the specimens heat treated for 24 h at 1150°C or annealed according to the two-step cycle

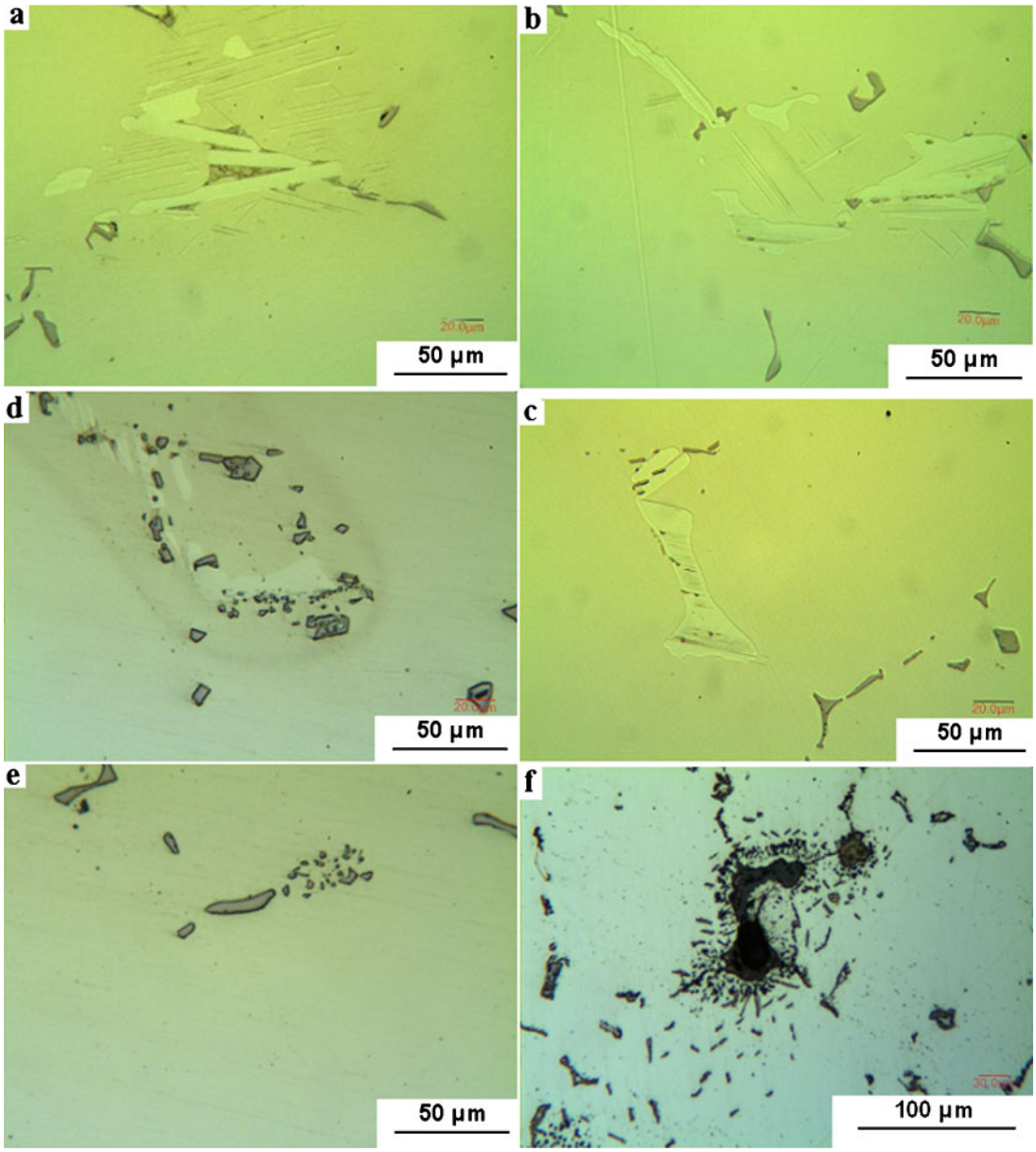

12 Microstructure of specimens annealed at *a* 1150°C for 4 h, *b* 1150°C for 16 h, *c* 1150°C for 24 h, *d* 1150°C for 24 h followed by 1200°C for 4 h, *e* 1150°C for 24 h followed by 1200°C for 10 h and *f* 1200°C for 10 h: all specimens were water quenched followed by mentioned annealing procedures

recommended in the present work could undergo all the five passes of rolling without any cracking to occur. This shows that even very small amounts of incipient melted regions impair hot workability of the IN939 superalloy. The difference observed between the second and the third sets of specimens was related to the absence of any η phase in the microstructure of the later strips (Fig. 13*e* and *f*). This resulted to more homogeneity of the microstructure and absence of any banding phenomenon in the final microstructure of the third set of specimens.

Conclusions

1. Elements Ti, Nb, Zr and Cr were segregated within the microstructure of IN939 alloy during its solidification. The three formers segregated positively, while the latter one segregated negatively. Al does not show significant segregation.

2. Annealing temperature for complete dissolution of the γ' particles in the thick cast parts was between 1100 and 1125°C.

3. Standard temperatures of solution annealing (i.e. 1150–1160°C) caused local (incipient) melting that occurs in the regions around the η phase.

4. The incipient melted regions enriched in Zr, Nb and B elements contained three different phases after water quenching.

5. Small amounts of incipient melted regions impair hot workability of the IN939 superalloy.

6. Long time annealing at 1150°C or using a two-step heat treatment can lead to significant improvement in hot workability of the alloy.

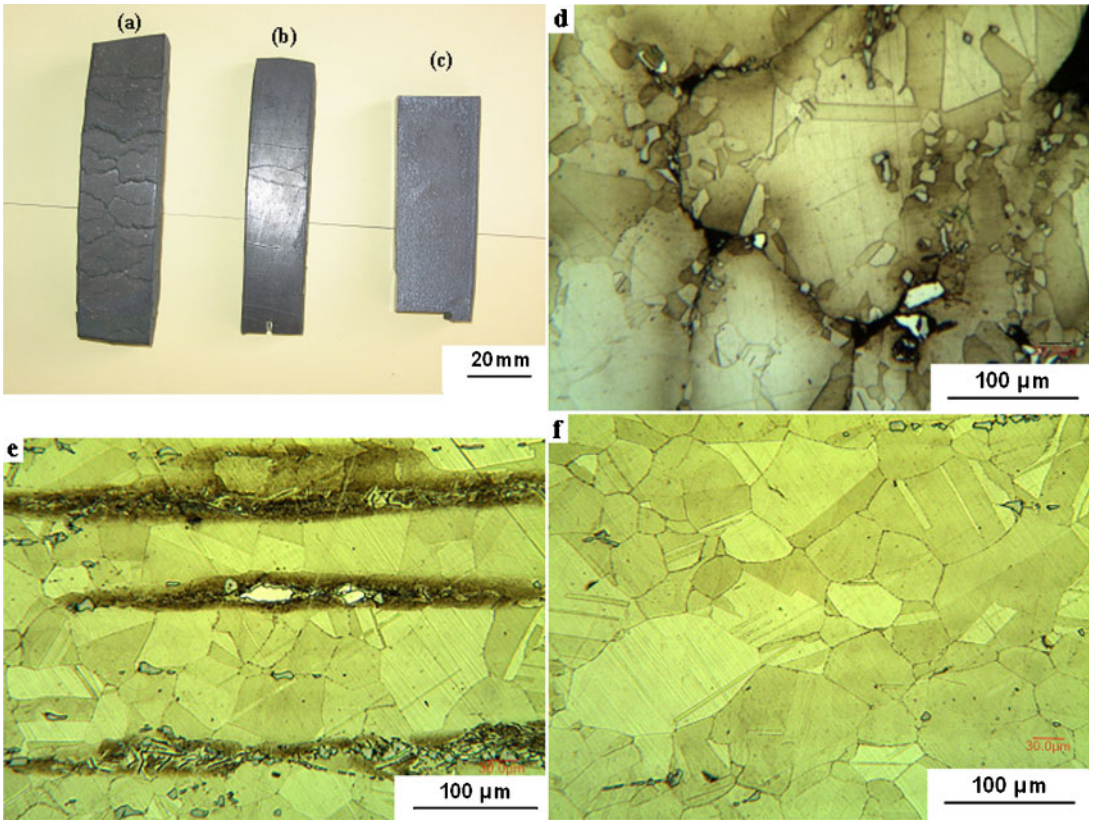

13 Rolled strips produced from large cross-section castings by *a* hot rolling of cast specimens after annealing at 1150°C for 4 h, *b* hot rolling of cast specimens after annealing at 1150°C for 24 h and *c* hot rolling of cast specimens after two-step homogenisation annealing proposed in the present work; *d* microstructure of strip in *a*, *e* microstructure of strip in *b*, and *f* microstructure of strip in *c*

References

1. C. T. Sims, N. S. Stoloff and W. C. Hagel: 'Superalloys II'; 1987, New York, John Wiley and Sons.
2. M. J. Donachie and S. J. Donachie: 'Superalloys: a technical guide', 2nd edn; 2002, Materials Park, OH, ASM International.
3. J. R. Davis: 'Heat resistant materials'; 1997, Materials Park, OH, ASM International.
4. R. C. Reed: 'The superalloys: fundamentals and applications'; 2006, Cambridge, Cambridge University Press.
5. T. B. Gibbons and R. Stickler: 'IN939 metallurgy, properties and performances', in 'High temperature alloys for gas turbines', (ed. R. Brunetaud *et al.*), 369–394; 1982, Liege, D. Reidel Publishing Company.
6. C. P. Cutler and S. W. K. Shaw: 'The interrelationship of γ' size, grain size and mechanical properties in IN939, a cast nickel-base superalloy', Proc. 5th Int. Conf. on 'Strength of metals and alloys', Aachen, Germany, August 1979, Pergamon, 1357–1362.
7. T. B. Gibbons, S. Osgerby, F. Gabrielli and V. Lupine: 'Factors controlling creep strength of cast Ni–Cr–bast alloys', *Mater. Sci. Technol.*, 1987, **3**, (4), 268–274.
8. M. T. Jovanovic, Z. Miskovic and B. Lukic: 'Microstructure and stress-rupture life of polycrystal, directionally solidified and single crystal casting on nickel based IN939 superalloy', *Mater. Charact.*, 1998, **40**, 261–268.
9. Z. Miskovic, M. Jovanovic, M. Gligic and B. Lukic: 'Microstructural investigation of IN 939 superalloy', *Vacuum*, 1992, **43**, (5), 709–711.
10. K. M. Delargy and G. D. W. Smith: 'Phase composition and phase stability of a high-chromium nickel-based superalloy IN939', *Metall. Trans. A*, 1983, **14A**, 1771–1783.
11. K. M. Delargy, S. W. K. Shaw and G. D. W. Smith: 'Effects of heat treatment on mechanical properties of high-chromium nickel-base superalloy IN939', *Mater. Sci. Technol.*, 1986, **2**, 1031–1037.
12. R. W. Hatala and J. J. Schirra: 'Development of a damage tolerant heat treatment for cast + hip Incoloy 939', in 'Superalloys 1996', (ed. R. D. Kissinger *et al.*), 137–143; 1996, Warrendale, PA, TMS.
13. S. W. K. Shaw: 'Response of IN939 to process variations, Superalloys', in 'Superalloys 1980', (ed. J. K. Tien *et al.*), 275–284; 1980, Champion, PA, TMS.
14. E. Balikci and D. Erdeniz: 'Multimodal precipitation in the superalloy IN738LC', *Metall. Mater. Trans. A*, 2010, **41A**, 1391–1398.
15. R. Rosenthal and D. R. F. West: 'Continuous γ' precipitation in directionally solidified IN738LC alloy', *Mater. Sci. Technol.*, 1999, **15**, 1387–1394.
16. D. Erdeniz and E. Balikci: 'Precipitate formation and evolution in the superalloy IN738LC', *Rare Met. Mater. Eng.*, 2009, **38**, (3), 142–146.
17. P. Li, S. S. Li and Y. F. Han: 'Influence of solution heat treatment on microstructure and stress rupture properties of a Ni_3Al base single crystal superalloy IC6SX', *Intermetallics*, 2011, **19**, (2), 182–186.
18. T. B. Gibbons: 'Superalloys in modern power generation applications', *Mater. Sci. Technol.*, 2009, **25**, (2), 129–135.
19. S. R. Hegde, R. M. Kearsey and J. C. Beddoes: 'Designing homogenization–solution heat treatments for single crystal superalloys', *Mater. Sci. Eng. A*, 2010, **A527**, (21–22), 5528–5538.
20. J. N. Dupont, C. V. Robino, J. R. Michael, M. R. Notis and A. R. Marder: 'Solidification of Nb-bearing superalloys. Part I: reaction sequences', *Metall. Mater. Trans. A*, 1998, **29A**, 2785–2796.
21. Z. Long, X. Liu, W. Yang, K. M. Chang and E. Barbero: 'Thermodynamic assessment of liquid composition change during solidification and its effect on freckle formation in superalloys', *Mater. Sci. Eng. A*, 2004, **A386**, 254–261.
22. P. D. Jablonski and C. J. Cowen: 'Homogenizing a nickel-based superalloy: thermodynamic and kinetic simulation and experimental results', *Metall. Mater. Trans. B*, 2009, **40B**, 182–186.
23. Z. J. Miao, A. D. Shan, J. Lu and H. W. Song: 'Segregation and diffusion characterisation in two-stage homogenisation of conventional superalloy', *Mater. Sci. Technol.*, 2011, **27**, (10), 1551–1557.
24. N. Warnken, D. Ma, A. Drevermann, R. C. Reed, S. G. Fries and I. Steinbach: 'Phase-field modelling of as-cast microstructure evolution in nickel-based superalloys', *Acta Mater.*, 2009, **57**, 5862–5875.
25. L. Yu, Y. Zhao, S. Yang, W. Sun, S. Guo, X. Sun and Z. Hu: 'As-cast microstructure and solidification behavior of a high Al- and Nb-containing superalloy', *J. Mater. Sci.*, 2010, **45**, 3448–3456.

26. D. L. Sponseller: 'Differential thermal analysis of nickel-base superalloys', in 'Superalloys 1996', (ed. R. D. Kissinger *et al.*), 259–270; 1996, Warrendale, PA, TMS.
27. L. A. Chapman: 'Application of high temperature DSC technique to nickel based superalloys', *J. Mater. Sci.*, 2004, **39**, 7229–7236.
28. N. D'Souza and H. B. Dong: 'Determination of transition temperatures during freezing and melting of interdendritic phases in Ni based superalloys', *Mater. Sci. Technol.*, 2011, **27**, (1), 325–331.
29. A. Formenti, A. Eliasson, A. Mitchell and H. Fredriksson: 'Solidification sequence and carbide precipitation in Ni-base superalloys IN718, IN625 and IN939', *High Temp. Mater. Process.*, 2005, **24**, (4), 239–258.
30. A. Cziraki, B. Fogarrasi, G. Van Tendeloo, P. Lamparter, M. Tegze and I. Bakonyi: 'Electron microscopy and X-ray diffraction studies of rapidly quenched Zr–Ni and Hf–Ni ribbons with about 90 at% Ni', *J. Alloy Compd*, 1994, **210**, 135–141.
31. Y. Xu: 'Experimental study of the structure of Ni–Zr metallic glasses', PhD thesis, McGill University, Montreal, Que., Canada, 1993.
32. H. Okamoto: 'Ni–Zr (nickel–zirconium)', *J. Phase Equilib. Diffus.*, 2007, **28**, 409.
33. K. P. Gupta: 'The Nb–Ni–Zr system (niobium–nickel–zirconium)', *J. Phase Equilib.*, 2000, **21**, (5), 485–493.
34. Z. J. Miao, A. D. Shan, J. Lu and H. W. Song: 'Microstructure and solidification behaviour characterisation of phosphorus and boron doped IN718 superalloy', *Mater. Sci. Technol.*, 2012, **28**, (3), 334–341.
35. S. Liling, W. Qi, Z. Zhiya and H. Zhuangqi: 'Effect of trace element B on microstructure of directionally solidified Co-base superalloy DZX40M', *Acta Metall. Sin.*, 1994, **7**, (1), 23–26.
36. O. A. Ojo and M. C. Chaturvedi: 'Liquation microfissuring in the weld heat-affected zone of an overaged precipitation-hardened nickel-base superalloy', *Metall. Mater. Trans. A*, 2007, **38A**, 356–369.
37. Z. J. Miao, A. D. Shan, Y. B. Wu, J. Lu, Y. Hu, J. L. Liu and H. W. Song: 'Effects of P and B addition on as-cast microstructure and homogenization parameter of Inconel 718 alloy', *Trans. Nonferr. Met. Soc. China*, 2012, **22**, 318–323.
38. J. Zhang and R. F. Singer: 'Effect of Zr and B on castability of Ni-based superalloy IN792', *Metall. Mater. Trans. A*, 2004, **35A**, 1337–1342.